Aerosol and Air Quality Research, 18: 1558–1572, 2018

ISSN: 1680-8584 print / 2071-1409 online
doi: 10.4209/aaqr.2017.09.0334

A Modeling Study of the Impact of Crop Residue Burning on $PM_{2.5}$ Concentration in Beijing and Tianjin during a Severe Autumn Haze Event

Yike Zhou[1,2], Zhiwei Han[2,3*], Ruiting Liu[2,3], Bin Zhu[1,4], Jiawei Li[2], Renjian Zhang[2]

[1] *Collaborative Innovation Center on Forecast and Evaluation of Meteorological Disasters, Nanjing University of Information Science and Technology, Nanjing 210044, China*
[2] *CAS Key Laboratory of Regional Climate-Environment for Temperate East Asia (RCE-TEA), Institute of Atmospheric Physics (IAP), Chinese Academy of Sciences (CAS), Beijing 100029, China*
[3] *University of Chinese Academy of Sciences, Beijing 100049, China*
[4] *Key Laboratory for Aerosol-Cloud-Precipitation of China Meteorological Administration, Nanjing University of Information Science and Technology, Nanjing 210044, China*

ABSTRACT

Crop residue burning is one of the important types of biomass burning in China and has potentially important effect on air quality and climate. A coupled meteorology and aerosol/chemistry model (WRF-Chem) with ground and satellite observations and biomass burning emission inventory were applied to investigate the spatial/temporal distribution and transport pathways of air pollutants and to quantify the contribution of crop residue burning to aerosol concentration in the North China Plain, with focus on Beijing and Tianjin during a severe haze episode on 7–11 October 2014, when the daily mean surface $PM_{2.5}$ concentration in Beijing reached 317 μg m^{-3}. During this period, intensive crop fires were detected over wide areas of eastern Henan, southern Hebei and western Shandong, and the crop residue burning emission was much larger than anthropogenic emission in major fire areas. Model comparison with ground observations demonstrated the WRF-Chem was able to generally reproduce surface meteorological variables and $PM_{2.5}$ concentration, although it tended to overpredict wind speed and aerosol concentration in some locations. Taking crop residue burning into account can apparently improve $PM_{2.5}$ prediction during the haze episode. The stagnant weather condition favored haze formation and maintenance in this region, and crop residue burning intensified haze pollution in both fire source and downwind regions. The crop residue burning emission on average contributed 19% to surface $PM_{2.5}$ concentration in Beijing during the haze episode, in which it contributed 40% and 29% to organic carbon aerosol and primary $PM_{2.5}$, respectively, and less to black carbon aerosol (4.9%). The impact of crop residue burning in Tianjin was smaller than that in Beijing, with an average contribution of 7.4% due to different fire sources and transport pathways.

Keywords: Crop residue burning; Beijing and Tianjin; Surface $PM_{2.5}$ concentration; Long range transport; FINN emission inventory; WRF-Chem simulation.

INTRODUCTION

Open biomass burning is one of the important sources of greenhouse gases, trace gases and particulate matter worldwide. Although episodic and highly variable, biomass burning can significantly influence atmospheric chemistry, air quality and climate on both global and regional scales (Crutzen and Andreae, 1990; Koppmann *et al.*, 2005; McMeeking *et al.*, 2006; Langmann *et al.*, 2009; Wang *et al.*, 2013; Tsay *et al.*, 2016). Chuang *et al.* (2016) ever revealed the long-range transport of biomass burning pollutants from Southeast Asia towards Central Mountain Range in Taiwan over East Asia in springtime and the mechanisms of high-altitude biomass burning plume descending to influence air quality on the ground. Crop residue burning, as one of the major types of biomass burning (Andreae and Merlet, 2001), emits large amounts of gases and particulate matter, which can worsen air quality, degrade visibility and damage human health under unfavorable weather conditions (Li *et al.*, 2007; Badarinath *et al.*, 2009; Gadde *et al.*, 2009; Mittal *et al.*, 2009; Tang *et al.*, 2013).

Many studies have been carried out to develop biomass burning emission inventory and to explore the influences of biomass burning on air quality and climate change. Zhang *et al.* (2014) investigated the uncertainties and differences in black carbon (BC) and organic carbon (OC) emissions and their radiative effects with seven biomass burning emission

*Corresponding author.
E-mail address: hzw@mail.iap.ac.cn; hzw@tea.ac.cn

inventories (FINN, GFED, etc.). By using FINN inventory with WRF-Chem model, Jiang *et al.* (2012) simulated the impacts of fire plumes on ozone concentration in Idaho and Montana during August 2007. In China, agricultural fires mostly occurred in central and north China in early/late June and October. In recent years, crop residue burning often induced serious air pollution in east China and drew increasing attention from public and scientific community (Yang *et al.*, 2008; Li *et al.*, 2010; Tao *et al.*, 2013; Mukai *et al.*, 2014; Long *et al.*, 2016; Yao *et al.*, 2016). A detailed agricultural open fire emission inventory over China with a spatial resolution of 1 km and temporal resolution of 10 days was developed by Huang *et al.* (2012), with the estimated annual emission of $PM_{2.5}$ being 0.27 Tg yr^{-1}. Wang *et al.* (2015) found that fire spots increased rapidly in North China in June during 2009 to 2012 and exerted large impact on aerosol optical depth and chemical compositions. Using levoglucosan as a molecular marker, Zhang *et al.* (2008) revealed that biomass burning was responsible for 18–38% of $PM_{2.5}$ organic carbon and for 14–32% of PM_{10} organic carbon during July 2002 to July 2003 in Beijing. Cheng *et al.* (2013) developed a new source identification method which used levoglucosan to K+ ratio in combination with levoglucosan to mannosan ratio and confirmed that biomass burning aerosol in Beijing mainly came from the combustion of crop residuals, also by using Positive Matrix Factorization (PMF) model they found about 50% of the OC and EC in Beijing were associated with biomass burning during summer and winter of 2011. Zhang *et al.* (2013) employed various approaches including positive matrix factorization (PMF) and potential source contribution function (PSCF) to explore seasonal contribution of various sources to $PM_{2.5}$ in Beijing and revealed that biomass burning contribution was about 12% averaged over the period between April 2009 and January 2010, with larger contribution in spring and autumn. Combining satellite retrievals, surface observations, and backward trajectory analysis, Zhu *et al.* (2010) investigated potential sources and transport pathways of air pollutants to Nanjing during a crop residue burning event. Cheng *et al.* (2014) indicated that biomass burning contributed 37% of $PM_{2.5}$ and 70% of organic carbon concentrations during a severe haze episode over the Yangtze River Delta region in early summer of 2011. Cheng *et al.* (2010) pointed out that crop residue fires in parts of eastern China can affect black carbon level at a remote site Tongyu in Jilin province of northeast China through long range transport, indicating a profound influence of agriculture fires on air quality in China. Li *et al.* (2017) reported that air quality in Northeast China can be potentially impacted by long-range transport of smoke aerosols from Eastern Siberia during the biomass burning season.

Despite the above studies, there is still limited research in quantifying the biomass burning influence on air quality in the Beijing-Tianjin-Hebei region, where severe haze pollution frequently occurred (Chen *et al.*, 2017; Yang *et al.*, 2017). In this study, ground and satellite observations together with WRF-Chem model are applied to investigate a severe haze event in Beijing and its surrounding areas during 7–11 October 2014. The meteorological characteristics, the spatial and temporal variations of open fires and air pollutants, the transport pathways and the impacts of crop residue fires on air quality in the North China Plain, with focus on Beijing and Tianjin are simulated and analyzed. This study is intended to quantitatively estimate the contribution of crop residue burning emission to aerosol concentration in this region by numerical model simulation, which could provide valuable insights into origin and mechanism of haze pollution.

MODEL CONFIGURATION AND PARAMETERS

The model used in this study is the Weather Research and Forecasting model coupled with Chemistry v3.5.1 (WRF-Chem v3.5.1), which is capable of simulating emission, transport, turbulent mixing and chemical transformation of aerosols and trace gases simultaneously with meteorological fields (Grell *et al.*, 2005). WRF-Chem for this study is configured to cover eastern part of China (Fig. 1), with 64(W-E) × 72(S-N) grid points at 27 km horizontal resolution (centering on 38°N, 117°E) and 30 vertical layers up to 50 hPa and 9 layers below 2 km. The physical options used in this study include the Lin microphysics scheme (Lin *et al.*, 1983), Grell cumulus scheme (Grell and Dévényi, 2002), RRTM longwave scheme (Mlawer *et al.*, 1997), Goddard shortwave scheme (Chou and Suarez, 1994), YSU PBL scheme (Hong and Pan, 1996) and Noah land surface scheme (Chen and Duhia, 2001). Photolysis rate used in photochemistry is calculated by Fast-J (Wild *et al.*, 2000). CBM-Z is used for gas phase chemistry (Zaveri and Peters, 1999). MOSAIC scheme is adopted to represent aerosol processes, in which aerosol size distribution is divided into four bins: 0.039–0.156 μm, 0.156–0.625 μm, 0.625–2.5 μm, 2.5–10 μm. Each bin includes sulfate, nitrate, ammonium, chloride, sodium, organic carbon, black carbon, other inorganic matter etc. (Zaveri *et al.*, 2008).

Anthropogenic emissions of $PM_{2.5}$, PM_{10}, OC, BC, CO, etc. are derived from the Multi-resolution Emission Inventory for China version 1.2 (MEIC v1.2) with the base year of 2012 and are monthly varied. We used the emission for October with a resolution of 0.25° × 0.25°, which is similar to the model grid resolution. Biogenic emission is from the Model of Emission of Gases and Aerosol from Nature (MEGAN) (Guenther, 2006). Six hourly, 1° × 1° NCEP reanalysis data is used to provide initial and boundary meteorological conditions. Boundary chemical conditions are from the Model for OZone And Related chemical Tracers version4 (MOZART-4). Model simulation is conducted from 28 September 2014 to 16 October 2014 with the first 3 days as spin-up time. Two numerical experiments are conducted in order to identify the crop residue burning effect. The baseline experiment (EXP_FINN) is designed to include all kinds of emissions, whereas the sensitivity experiment (EXP_NOFIRE) is identical to base case except crop burning emission is closed.

Open biomass burning emissions are obtained from the Fire INventory from NCAR (FINNv1.5) (http://bai.acom.ucar.edu/Data/fire/). FINN applies MODIS satellite retrievals of active fire and land cover, together with fuel loadings

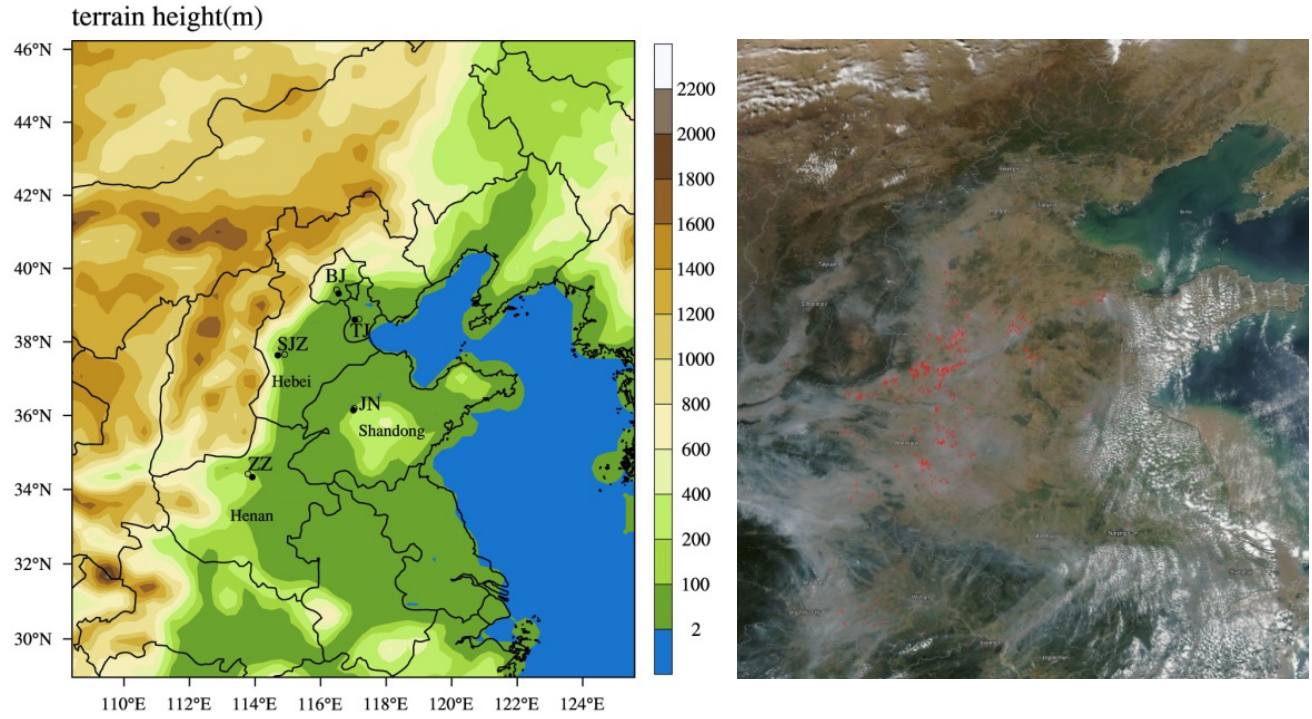

Fig. 1. (a) The study domain, terrain height (m) and surface observation sites (BJ: Beijing; TJ: Tianjin; SJZ: Shijiazhuang; JN: Jinan; ZZ: Zhengzhou). Meteorological observation sites are denoted by filled circles and $PM_{2.5}$ concentration observation sites are denoted by circles. (b) MODIS true color image with fire spots on 6 October.

and emission factors to provide daily and 1 km resolution biomass burning emission estimates for use in regional and global chemical transport models. This inventory provides global estimates of a number of chemical species with high temporal and spatial resolution. The emission E_i of species i is calculated by the following equation (Wiedinmyer *et al.*, 2006, 2011):

$$E_i = A(x,t) \times B(x) \times FB \times ef_i \quad (1)$$

where A is the area burned at time t and location x, B is the biomass loading at location x, FB is the fraction of biomass that is burned in fire and ef_i is the emission factor of species i. The emission factor ef_i for $PM_{2.5}$, OC, BC, CO, NO_x, NH_3, SO_2 is set to 5.8, 3.3, 0.69, 111, 3.5, 2.3, 0.4 g kg^{-1}, respectively, based on previous studies (Andreae and Merlet, 2001; Akagi *et al.*, 2011) due to the limitation of such information in China. The possible uncertainties in the emission estimation could be associated with fire identification, land cover classification, fuel loading and consumption, as well as emission factors. The diurnal variation of biomass emission is prescribed with peak value in the afternoon (14:00) and zero in the evening and linearly interpolated to the other hours in the daytime.

Surface observations of meteorological variables including sea level pressure, wind speed, air temperature and relative humidity in Beijing, Tianjin, Shijiazhuang, Jinan, Zhengzhou are obtained from China Meteorological Data Sharing Service System (http://cdc.cma.gov.cn). Hourly surface concentration of $PM_{2.5}$ is from the surface observation of China National Environmental Monitoring Center (http://106.37.208.233:20035/). Site locations are presented in Fig. 1(a).

MODEL RESULTS AND DISCUSSION

Haze Event and Crop Fires

A severe and 5-days lasting haze event occurred in Beijing during 7–11 October 2014. The first orange alert in the second half of 2014 was released on 9 October by the Heavy Air Pollution Emergency Command Office of Beijing. Most of the North China Plain and parts of eastern China were also influenced by the haze event. Crop fires were detected in central China around this period by MODIS satellite, which were clearly shown in Fig. 1(b).

Figs. 2(a)–2(d) shows the locations of active fires during 5–8 October from FINN. It is striking that a number of fire hot spots appeared in the southern Hebei, eastern Henan and western Shandong provinces on 5 October (Fig. 2(a)), and the number of fires increased remarkably and expanded to surrounding areas on 6 October (Fig. 2(b)). On 7 (Fig. 2(c)) and 8 (Fig. 2(d)) October, the number of fires decreased gradually. The total number of fires in domain is counted to be 156, 498, 300, 150 on 5–8 October, respectively.

Relative Magnitudes of MEIC and FINN Emissions

It is interesting to know the relative magnitude of anthropogenic and crop residue burning emissions during the study period. Both MEIC and FINN are latitude-longitude based inventory and they are interpolated to the WRF-Chem lambert projection by using the same method.

Fig. 3 shows the spatial distribution the of the total emission amounts of primary $PM_{2.5}$, OC, BC from MEIC and FINN

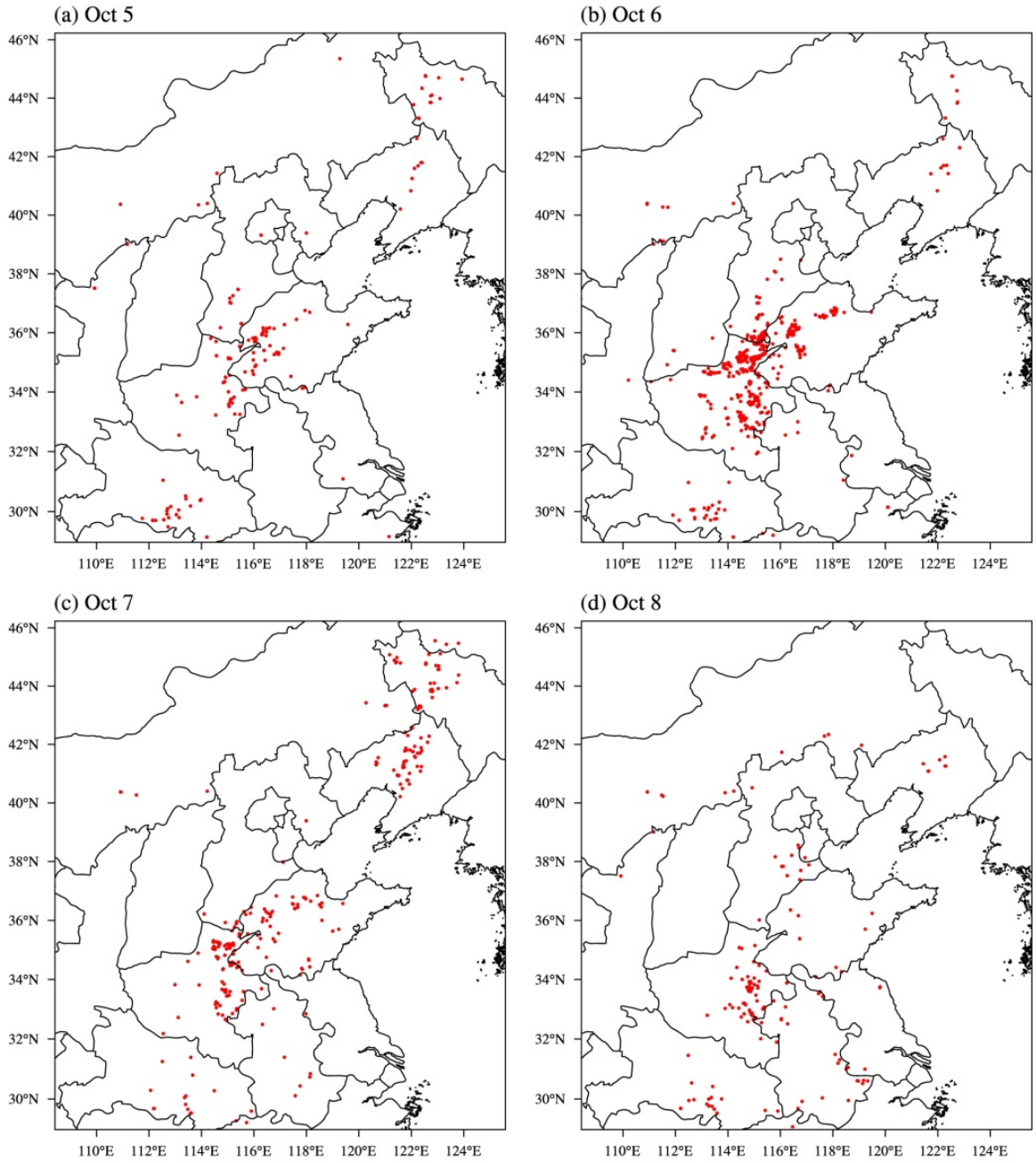

Fig. 2. (a–d) The locations of MODIS cumulative fires during 5–8 October.

during 5–8 October, respectively, when most fires occurred during this period. Anthropogenic emissions (MEIC) mainly distributed over east China, with large values over wide areas extending from the Beijing-Tianjin-Hebei (BTH) region, across parts of central China to the Yangtze River Delta (Figs. 3(a)–3(c)). Crop burning emissions were concentrated in northern Henan, southern Hebei and western Shandong, with the largest fire emission in northeastern Henan (Figs. 3(d)–3(f)). It was striking that the crop burning emissions of primary $PM_{2.5}$ and OC in the main fire areas, such as eastern Henan, were much larger than anthropogenic emissions (Figs. 3(d) and 3(e)), suggesting the potentially important influence on downwind air quality. The crop burning emission for BC was comparable to that from anthropogenic origin. The crop residue fires over southern Hubei and northeastern China have little impacts on Beijing due to relatively weak emission and longer distance. The region (31.5–42.5°N, 110.5–120°E) with main fire spots and high aerosol concentrations is marked with the black enclosed line in Fig. 3(a), and the total emissions of aerosols ($PM_{2.5}$, OC, BC) and gases (CO, NO_x, NH_3, SO_2) from MEIC and FINN in this region during 5–8 October are presented in Table 1. The crop burning emissions of $PM_{2.5}$, OC, BC, CO, NO_x, NH_3, SO_2 are estimated to be 9.9, 4.5, 0.3, 80.4, 2.0, 1.6, 0.7 Gg, respectively. The ratio of biomass burning to anthropogenic emissions can be as large as 56% for primary

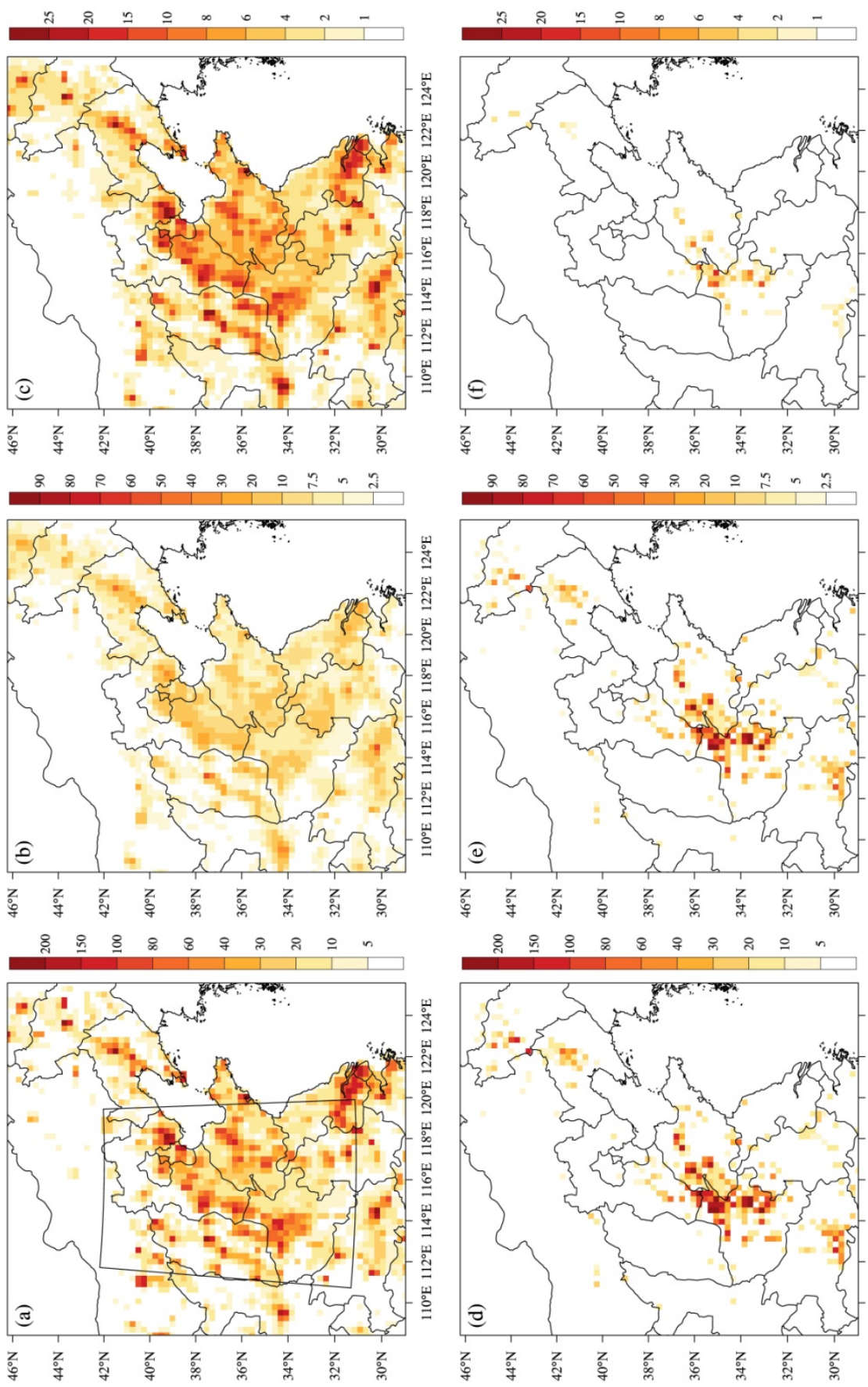

Fig. 3. Spatial distribution of total emission amounts of (a, d) primary $PM_{2.5}$, (b, e) OC, and (c, f) BC from (a, b, c) MEIC and (d, e, f) FINN during 5–8 October (unit: ton grid^{-1}).

Table 1. Total emissions (Gg) in the domain (31.5–42.5°N, 110.5–120°E) during 5–8 October 2014.

	MEIC	FINN	FINN/MEIC
$PM_{2.5}$	26.6	9.9	0.37
OC	8.0	4.5	0.56
BC	5.8	0.3	0.05
CO	549.5	80.4	0.15
NO_x	105.0	2.0	0.02
NH_3	29.4	1.6	0.05
SO_2	101.9	0.7	0.01

OC, followed by 37% for primary $PM_{2.5}$ and 15% for CO, with ratios less than 5% for other species.

Weather Condition

Weather maps at the surface and 500hPa at 08:00 LST on 7, 9, 11 October are presented in Fig. 4. On 7 October (Figs. 4(a) and 4(b)), surface synoptic pattern was characterized by a deep trough over northeast China and high pressures over the Beijing-Tianjin region and Korean peninsula, in combination with prevailing northwesterly winds at 500 hpa over north China, which resulted in southerlies over the North China Plain and was favorable for accumulation of air pollutants. On 9 October (Figs. 4(c) and 4(d)), the trough moved southeastwards, and the high pressures were persistent in the above region, which could further enhance pollutant levels. On 11 October (Figs. 4(e) and 4(f), a cold front associated with a strong high pressure system appeared in north China, moving southeastward and approaching the Beijing-Tianjin-Hebei region, with light rain occurred around Beijing.

Model Evaluation

Fig. 5 shows the observed and simulated daily mean 2 m-air temperature, 2 m-relative humidity (RH), 10 m-wind speed, and surface $PM_{2.5}$ concentration in Beijing and Tianjin during 1–15 October 2014, respectively. In general, the model simulations (EXP_FINN) agree well with observations except for slight overprediction of air temperature and consequently underprediction of relative humidity. The model is able to well reproduce the temporal variation of meteorological variables and $PM_{2.5}$ concentrations, exhibiting the increases of air temperature and RH along with the decrease of wind speed and the increase of $PM_{2.5}$ level during 6–12 October. It's clearly seen that the observed $PM_{2.5}$ concentration increased abruptly from 33.0 μg m^{-3} on 6 October to a peak value of 316.7 μg m^{-3} on 9 October, and decreased to 17.8 μg m^{-3} on 12 October, the model reproduced the day-to-day variation quite well in both haze and non-haze days except for overprediction by about 50 μg m^{-3} on 7–8 October. The variation of $PM_{2.5}$ concentration in Tianjin resembled that in Beijing except that the maximum value (~170 μg m^{-3}) was lower, and the model tended to slightly overpredict observation during the study period.

The statistics for model predictions in comparison with observations for 3-hourly air temperature and relative humidity at 2 m, wind speed at 10 m and hourly surface $PM_{2.5}$ concentration at the five sites: Beijing (BJ), Tianjin (TJ), Shijiazhuang (SJZ), Jinan (JN) and Zhengzhou (ZZ) during 1–15 October 2014 are listed in Table 2. The WRF-Chem reproduces air temperature quite well, with R and NMB in the ranges of 0.9–0.96 and –9.8–1.8%, respectively at these sites, whereas the model tends to underpredict RH (NMBs of –20.5–0.8%) with R of 0.84–0.93. The model consistently predicts higher wind speed by 12.1–100% at the five sites, with relatively lower R of 0.44–0.71. It is also noticed that the maximum overprediction (by a factor of two) is under small wind condition (1.2 m s^{-1}) at SJZ, the overall the overprediction of wind speed at all the sites could be due to model uncertainties in representing urban surface characters and in boundary layer schemes. Among the sites, Beijing and Tianjin exhibit better performances for meteorological variables, with least biases in wind speed (12%) and surface air temperature (1.3%). The model predicted higher $PM_{2.5}$ concentration at all sites, with NMBs from 5.8% to 38.9% with R of 0.54–0.86. The model reproduced daily $PM_{2.5}$ concentration best in Beijing with the highest R (0.86) and the least bias (5.8%) among the sites, followed by that in Tianjin (R of 0.73, NMB of 19.9). The overprediction of $PM_{2.5}$ concentration could be attributed to the coarser model grid size which can't well reflect local inhomogeneous land use, the uncertainties in emission inventory or the stronger transport effect from adjacent areas due to overprediction of wind speed. It is also noticed that the observed $PM_{2.5}$ concentrations averaged over the study period was highest in SJZ (142.8 μg m^{-3}), followed by Beijing (117.9 μg m^{-3}) and Zhengzhou (109.9 μg m^{-3}), and the lowest in Jinan (76.6 μg m^{-3}), the model generally reproduced the spatial distribution of the mean $PM_{2.5}$ concentration during this period. The statistics over all the five sites exhibit a fairly good performance of the WRF-Chem in the study domain, with R of 0.94,0.89, 0.6 and 0.66 for air temperature and relative humidity at 2 m, wind speed at 10m and surface $PM_{2.5}$ concentrations, and the corresponding NMBs of –2.4%, –12.6%, 33.3% and 19.7%, respectively.

Regional Transport of Air Pollutants by South Winds

Fig. 6 shows the spatial distribution of daily mean surface $PM_{2.5}$ concentration and wind vector at 10 m during 6–9 October, respectively. On 6 October (Fig. 6(a)), surface $PM_{2.5}$ concentration was mostly less than 80 μg m^{-3} in Beijing-Tianjin and northern Hebei province, and higher than 120 μg m^{-3} in southern Hebei and eastern Henan provinces, where crop residue fire began to be active, the maximum value can reach 260 μg m^{-3}, resulting from a combined effects of anthropogenic and crop burning in those areas. On 7 October (Fig. 6(b)), a pollution plume appeared extending from northeastern Henan, crossing southern Hebei to Beijing-Tianjin and further to northern Hebei in conjunction with prevailing southerlies, with $PM_{2.5}$ concentration increasing to 280 μg m^{-3} in the region, reflecting the northward transport of pollutants from fire source regions. The wind speed in Beijing was decreased compared to 6 October, implying possible accumulation of local pollutants and suggesting a combined effects of both local emission and regional transport from upwind emissions, such as southern Hebei

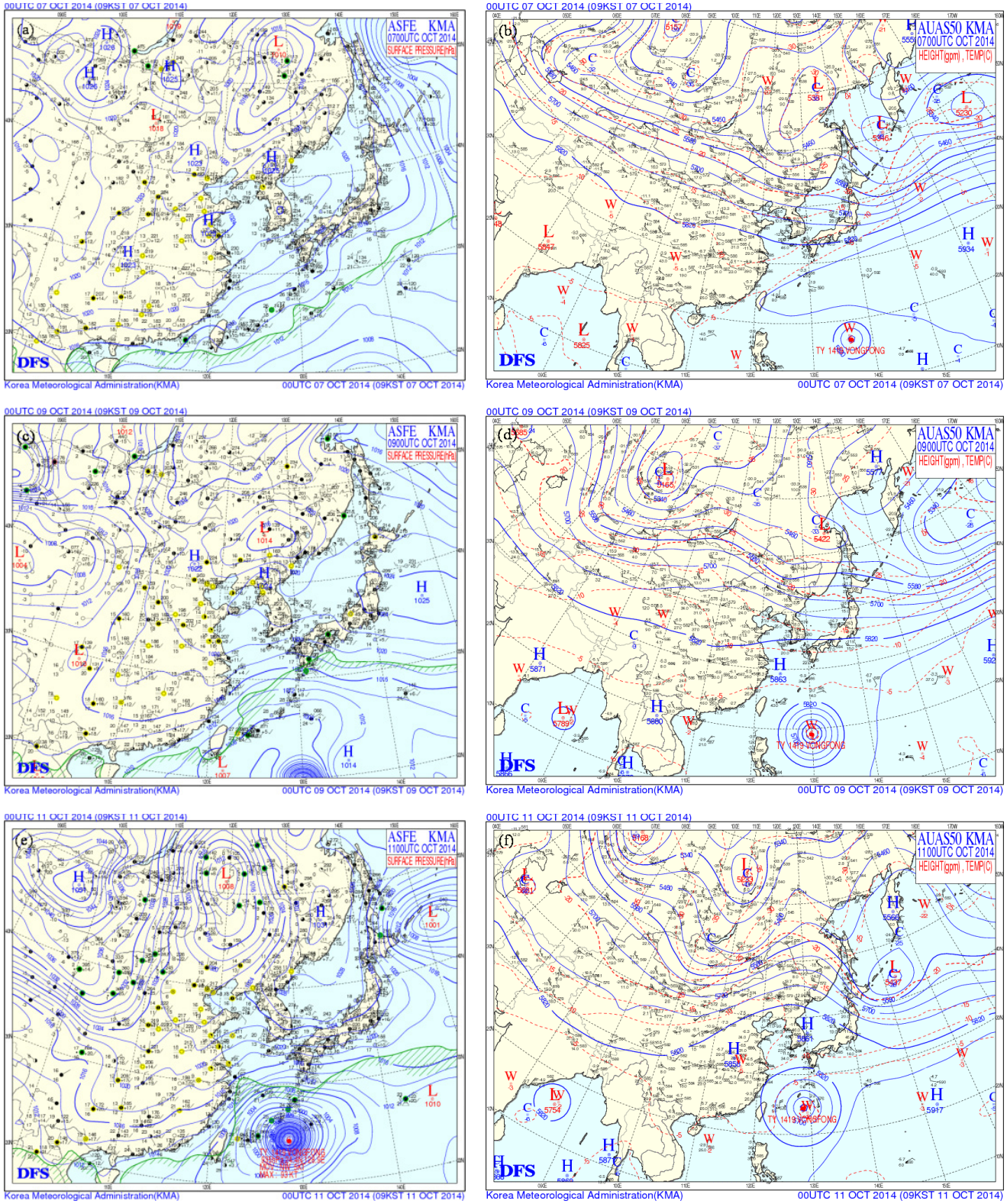

Fig. 4. Weather maps at the (left) surface and at (right) 500 hpa at 08:00 LST on 7, 9, 11 October 2014.

and eastern Henan provinces. On 8 October (Fig. 6(c)), the surface $PM_{2.5}$ concentration further increased, especially in the areas from Shijiazhuang to Beijing-Tianjin and parts of northern Hebei, with the maximum of 300 μg m^{-3} in southern parts of Beijing. On 9 October, the $PM_{2.5}$ level in southern Hebei and eastern Henan decreased (Fig. 6(d)), which was consistent with the decreasing trend of fires as shown in Fig. 2(d). However, in parts of northeastern Hebei, $PM_{2.5}$ concentration increased to a similar level to that in Beijing. It was noticed in Fig. 6 that the wind flows were

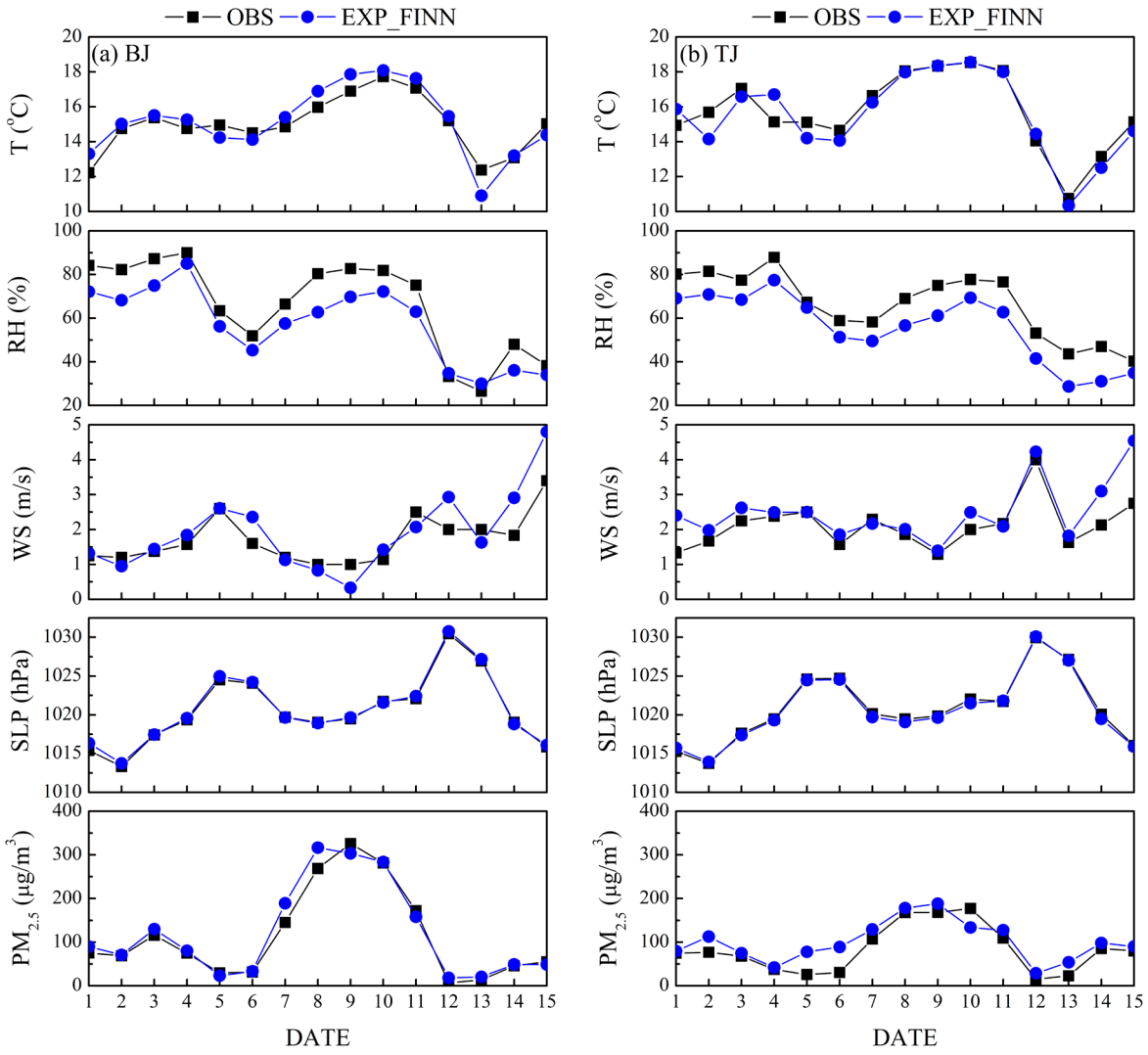

Fig. 5. The observed and simulated daily mean sea level pressure (SLP, hPa), air temperature at 2 m (T,°C), relative humidity (RH,%) at 2 m, wind speed at 10 m (WS, m s^{-1}) and surface $PM_{2.5}$ concentration ($PM_{2.5}$, μg m^{-3}) in (a, left) Beijing and (b, right) Tianjin during 1–15 October 2014.

alike during 7–9 October, indicating the stable atmospheric stability and air flow favorable for haze formation and regional transport. In addition, Beijing is surrounded by mountains at east-north-west three directions, which was also unfavorable for pollutant diffusion.

Contribution of Crop Residue Burning to Surface $PM_{2.5}$ Concentration

The model simulated spatial distribution of surface $PM_{2.5}$ concentration averaged over 7–11 October without and with crop residue burning emission are shown in Fig. 7, respectively, to identify the crop burning contribution. The simulated 5-day average $PM_{2.5}$ concentrations from anthropogenic emission (Fig. 7(a)) (EXP_NOFIRE) exceeded the NAAQS (National Ambient Air Quality Standards) daily mean $PM_{2.5}$ of 75 μg m^{-3} over wide areas of east China, with the most polluted regions in Beijing,Tianjin and Hebei province, where the maximum value reached 240 μg m^{-3}. The contribution of crop residue burning to surface $PM_{2.5}$ concentration are calculated by subtracting the model result of EXP_NOFIRE from those of EXP_FINN. While taking crop burning emission into account, $PM_{2.5}$ concentration was considerably elevated especially in Henan and Hebei provinces, with the maximum exceeding 260 μg m^{-3} in Shijiazhuang, northeastern Hebei and parts of Beijing (Fig. 7(b)). Fig. 7(c) clearly shows the $PM_{2.5}$ concentrations increased by ~50 μg m^{-3} over large areas from central China to the North China Plain, with the maximum increase in northeastern Henan and southern Hebei, where intensive fires occurred (shown in Fig. 3(d)) and about 42 μg m^{-3} increase in the southern areas of Beijing. The percent increase of $PM_{2.5}$ concentration induced by crop burning emission (Fig. 7(d)) exceeded 40% in the major fire regions (northern Henan and southern Hebei) and reached 22% in Beijing due to long range transport, whereas that in Tianjin (~10%) is apparently lower than in Beijing, which will be discussed in the following section.

The model simulated daily mean surface concentrations

Table 2. Statistics for model predictions for 3-hourly 2 m-temperature (T, °C), 2 m-relative humidity (RH, %), 10 m-wind speed (WS, m s^{-1}), hourly surface $PM_{2.5}$ concentration (μg m^{-3}) at the 5 sites during 1–15 October. MB: mean bias, NMB: normalized mean bias, R: correlation coefficient.

		N	OBS	EXP_FINN			
			MEAN	MEAN	MB	NMB (%)	R
BJ	T	118	15.0	15.2	0.2	1.3	0.94
	RH	118	65.8	57.2	–8.6	–13.1	0.93
	WS	87	1.74	1.95	0.21	12.1	0.70
	$PM_{2.5}$	325	117.9	124.7	6.8	5.8	0.86
TJ	T	117	15.7	15.5	–0.2	–1.3	0.96
	RH	117	65.9	55.5	–10.4	–15.8	0.92
	WS	107	2.14	2.54	0.4	18.7	0.71
	$PM_{2.5}$	344	83.9	100.6	16.7	19.9	0.73
SJZ	T	118	16.4	16.7	0.3	1.8	0.90
	RH	118	68.7	54.6	–14.1	–20.5	0.86
	WS	57	1.2	2.4	1.2	100	0.44
	$PM_{2.5}$	349	142.8	162.8	20.0	14.0	0.59
JN	T	117	17.3	15.6	–1.7	–9.8	0.95
	RH	117	55.0	55.4	0.4	0.7	0.92
	WS	109	1.9	2.6	0.7	36.8	0.48
	$PM_{2.5}$	351	76.7	106.5	29.8	38.9	0.57
ZZ	T	118	18.7	18.2	–0.5	–2.7	0.93
	RH	118	62.1	54.7	–7.4	–11.9	0.84
	WS	89	1.8	2.6	0.8	44.4	0.67
	$PM_{2.5}$	345	109.9	141.1	31.2	28.4	0.54
TOTAL	T		16.6	16.2	–0.4	–2.4	0.94
	RH		63.5	55.5	–8.0	–12.6	0.89
	WS		1.8	2.4	0.6	33.3	0.60
	$PM_{2.5}$		106.2	127.1	20.9	19.7	0.66

of $PM_{2.5}$ in Beijing and Tianjin and concentrations of $PM_{2.5}$ organic carbon, $PM_{2.5}$ black carbon in Beijing with (EXP_FINN) and without (EXP_NOFIRE) crop residue burning emission during 1–15 October 2014 are presented in Fig. 8. The observed maximum $PM_{2.5}$ concentration reached 316.7 μg m^{-3} on 9 October in Beijing (Fig. 8(a), the corresponding simulations from EXP_FINN and EXP_NOFIRE were 301.5 μg m^{-3} and 252.8 μg m^{-3} respectively. The $PM_{2.5}$ concentrations averaged over the haze period of 7–11 October were 238.6 μg m^{-3}, 246.8 μg m^{-3} and 206.8 μg m^{-3} from observation, EXP_FINN and EXP_NOFIRE, respectively. It demonstrated the simulated $PM_{2.5}$ values by considering crop residue burning emission were apparently closer to observation and the necessity to include the crop burning emission sector in air quality model simulation. The difference in $PM_{2.5}$ concentration between the two experiments in Tianjin was much smaller (Fig. 8(b)) than that in Beijing. On 9 October, the crop residue burning contributed 48.7 μg m^{-3} (with percentage of 19.3%) to surface $PM_{2.5}$ concentration in Beijing, whereas such contribution (10.3 μg m^{-3}, 5.8%) in Tianjin was much smaller. The total $PM_{2.5}$ concentration is the sum of primary $PM_{2.5}$ (except OC and BC), OC, BC, inorganic aerosols and so on. It was found the largest change in aerosol components of $PM_{2.5}$ in Beijing induced by crop residue burning was organic carbon aerosol, which changed from 16.7 μg m^{-3} to 23.3 μg m^{-3}, increasing by about 40%, the second was primary $PM_{2.5}$, which increased from 52.3 μg m^{-3} to 67.4 μg m^{-3} (29% percent increase), indicating the significant contribution of crop burning to the two type of aerosol species. The changes in concentrations of black carbon, sulfate and nitrate was relatively small, about 7%, 14% and 15% respectively due to their relatively small crop burning emission compared with anthropogenic sources (Table 1). Averaged over the whole haze period of 7–11 October, the percent contributions from crop residue burning to surface concentrations of total $PM_{2.5}$, primary $PM_{2.5}$, OC, BC, sulfate and nitrate in Beijing were estimated to be 19%, 25.4%, 37.2%, 4.9%, 11.3% and 16.4% respectively. It was noteworthy that the contributions of crop residue burning emission to $PM_{2.5}$ concentration during the whole haze period and on the most severe day (9 October) were almost the same, indicating the continuous transport of crop fire emitted species to Beijing under stable southerlies during this period. Zhang *et al.* (2013) estimated the contribution of biomass burning to surface $PM_{2.5}$ concentration in Beijing to be 17% in autumn by using PMF method, the result from this study (19%) was consistent with but somewhat larger than theirs due to different time period.

It was noteworthy that the effect of crop residual fire on $PM_{2.5}$ concentration was much lower in Tianjin than that in Beijing (7.4% vs 19% in terms of period mean) although both cities located downwind of the fire sources and were just 120 km apart. It's interesting to explore the reasons for the different impact of crop residual burning. For this purpose, the 48 hours backward trajectories arriving at Beijing

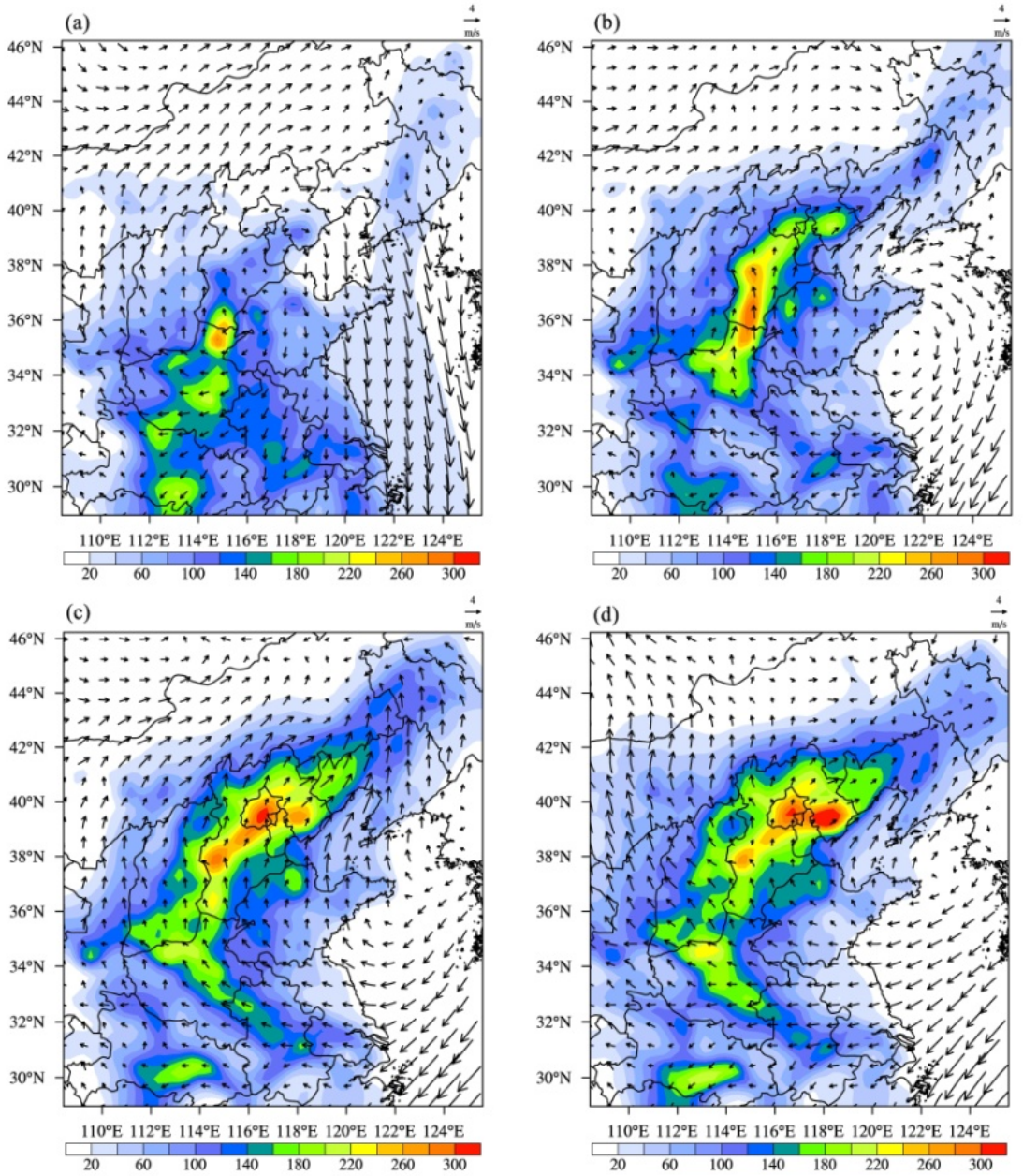

Fig. 6. (a–d) Spatial distribution of the daily mean surface $PM_{2.5}$ concentrations and 10 m wind vectors on 6–9 October.

(39.9°N, 116.3°E) and Tianjin (39.12°N, 117.2°E) at 14:00 LST on 8 October 2014 for three altitudes were calculated by using HYSPLIT4.9. Fig. 9 shows the backward trajectories at three altitudes (100 m, 500 m, 1000 m) overlapped with fire spots on 6 October, when the number of fires reached maximum (Fig. 2(b)). It clearly shows that the trajectories from Beijing (Fig. 9(a)) at altitudes of 100 m and 500 m right passed the southern Hebei and eastern Henan on 6–7 October, when most intensive fires occurred in those areas, indicating the long range transport of chemical species from the crop residual fires to Beijing along with the moderate south wind in 1–2 days. The trajectory at 1000 m altitude did not pass the fire areas, implying the transport of crop burning induced pollutants were confined within the lowest several hundred meters above ground. The backward trajectories from Tianjin (Fig. 9(b)) at 100 m and 500 m just passed western Shandong province, where relatively less fires occurred, and although the trajectory at 1000 m passed through a part of eastern Henan province, which is one of the major fire spots, the surface sources were difficult to rise to this level to be transported downwind, therefore the influence of crop fire on air quality in Tianjin was much smaller than that in Beijing.

In summary, the haze event in Beijing, as well as in Tianjin and Hebei province was mainly attributed to accumulation of aerosols from anthropogenic emission under unfavorable weather conditions (stable atmosphere and weak diffusivity together with small wind), the crop residual burning in parts of central China (southern Hebei, eastern Henan and western Shandong) aggravated the regional

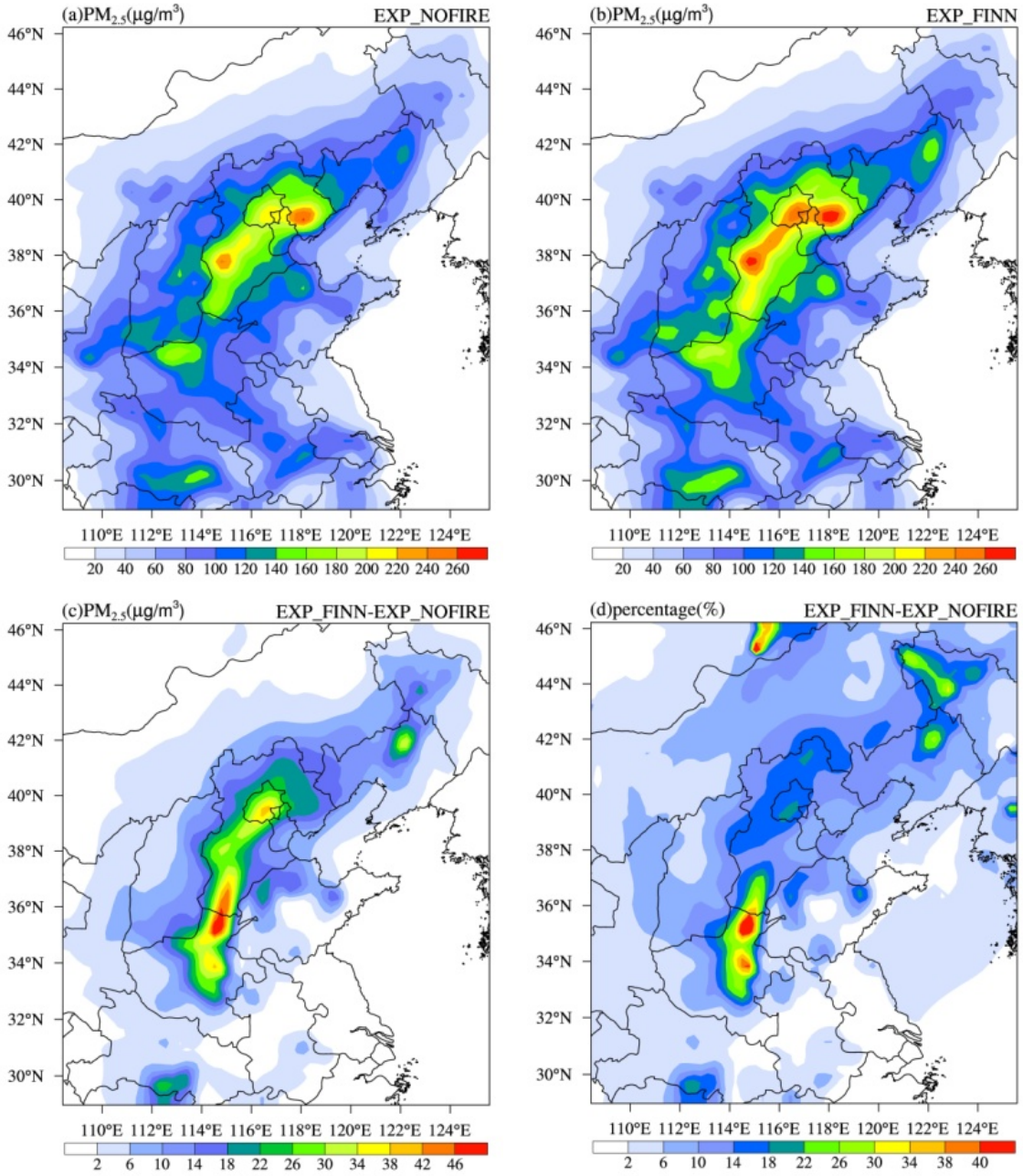

Fig. 7. Spatial distributions of surface $PM_{2.5}$ concentration (μg m^{-3}) without (a. EXP_NOFIRE) and with (b. EXP_FINN) crop residue burning emission, and the (c) contribution, and (d) contribution in percentage to surface $PM_{2.5}$ concentration of the crop residue burning averaged over the period of 7–11 October.

haze pollution by emitting large amounts of pollutants and persistent northward transport of fire-emitted pollutants under continuous and weak southerlies, which accounted for about 20% of surface $PM_{2.5}$ concentration in Beijing during the 5-day haze episode.

CONCLUSION

In this study, by applying the WRF-Chem model, FINN biomass burning emission inventory, ground and satellite observations, as well as back trajectory analysis, a severe haze event over the north China Plain during 7–11 October 2014 was investigated with focus on the impact of crop residue fire on surface $PM_{2.5}$ concentrations in fire source and downwind areas and the transport pathways of fire emitted aerosols under typical weather condition. Model validation showed the WRF-Chem model generally reproduced the spatial and temporal distribution of meteorological variables and $PM_{2.5}$ concentrations, and it demonstrated that the inclusion of crop residue burning emission considerably improved model prediction of $PM_{2.5}$ concentrations in Beijing.

The haze period was characterized by stagnant air, small south wind and vertical diffusivity associated with weak

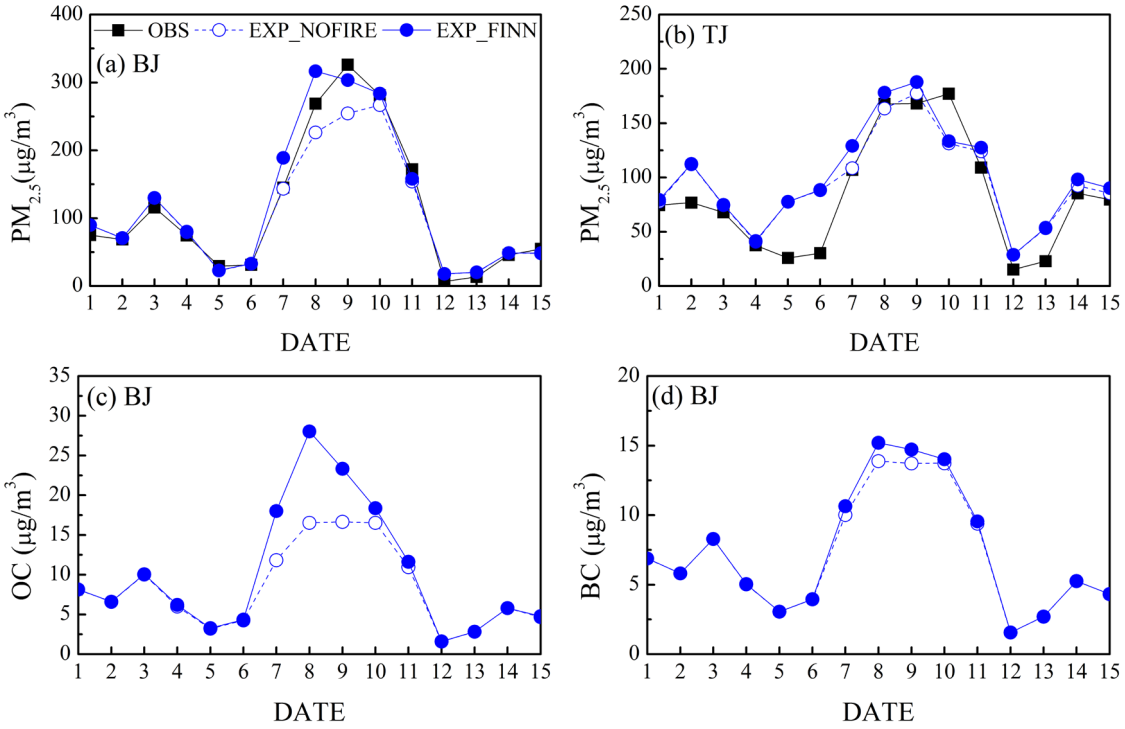

Fig. 8. The model simulated daily mean surface concentrations (μg m^{-3}) of $PM_{2.5}$ (a) in Beijing, (b) in Tianjin, (c) $PM_{2.5}$ organic carbon concentration in Beijing, and (d) $PM_{2.5}$ black carbon concentration in Beijing with (dot) and without (open circle) crop residue burning emission during 1–15 October. The observed $PM_{2.5}$ concentrations are also presented for Beijing.

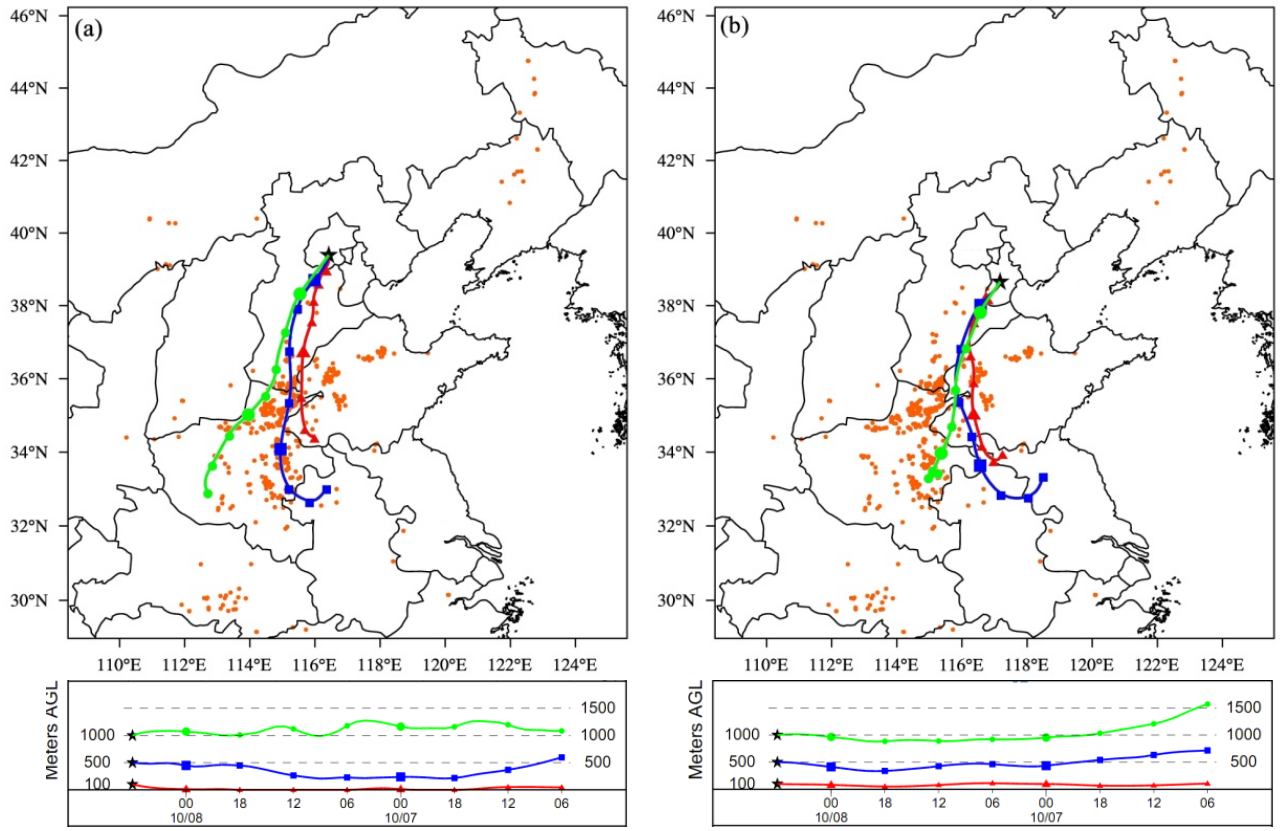

Fig. 9. 48 hours backward trajectories arriving at (a) Beijing and (b) Tianjin at 14:00 LST on 8 October 2014 for three altitudes of 100 m (red line), 500 m (blue line) and 1000 m (green line), orange dots denote fire spots on 6 October), bottom panels denote the vertical profiles of the three trajectories.

and persistent high pressures which favored haze formation and maintenance and caused high daily $PM_{2.5}$ concentration up to 317 μg m^{-3} in Beijing. During this period, crop residue fires occurred over wide areas of southern Hebei, eastern Henan and western Shandong, with maximum numbers of fires on 6 October. It was striking that the crop residue burning emission can be comparable in magnitude to anthropogenic emissions in terms of regional mean (31.5–42.5°N, 110.5–120°E) and significantly larger than anthropogenic emissions in the crop fire areas. The total crop emission amounts in the above region during 5–8 October are estimated to be 9.9, 4.5, 0.3, 80.4, 2.0, 1.6, 0.7 Gg for $PM_{2.5}$, OC, BC, CO, NO_x, NH_3, SO_2, respectively. The mean ratios of crop burning to anthropogenic emissions can be as large as 56% for primary OC, followed by 37% for primary $PM_{2.5}$ and 15% for CO, with less than 5% for other species.

The model results revealed the crop residue fires considerably affected $PM_{2.5}$ level not only in fire source region but also in downwind areas as far as Beijing by long range northward transport. It was estimated that the crop burning percent contribution to surface $PM_{2.5}$ level can exceed 40% in the major fire areas of northern Hebei and eastern Henan, and reach almost 20% in downwind Beijing. The percent contribution of crop residue burning emission to $PM_{2.5}$ concentration in Beijing during the haze episode on 7–11 October was estimated to be 19%, in which its contributions to organic carbon aerosol (40%) and primary $PM_{2.5}$ (29%) were largest among the $PM_{2.5}$ components, followed by nitrate (16.4%), sulfate (11.3%) and black carbon (4.9%). It was noteworthy that the impact of crop residue fires on Tianjin was much smaller than that in Beijing, with the 5-day average percent contribution of 7.4%, which was due to the effects of different fire sources. The back trajectories starting from Tianjin mainly passed over less fire areas in western Shandong, whereas those from Beijing passed right over the major fire spots in eastern Henan, resulting in different extent of the crop residue burning influence. The results from this study demonstrated the considerable impact of crop residue burning on air quality over the wide areas of the north China Plain from the major fire areas to most of Hebei province and Beijing. Although the model prediction of $PM_{2.5}$ is apparently improved by considering crop residue burning, the model result is still subject to some limitations. First, the satellite data over fire areas is very limited (only two times per day) and is affected by cloud, which could lead to underestimation of FINN emission. Second, the diurnal variation of FINN emission is calculated by linear interpolation between the satellite retrievals in daytime and the assumed zero at nighttime, which is not realistic because fire may also occur at night. Third, the emission factors for chemical species used in FINN are prescribed based on previous studies, which could not well represent crop residue burning in east China. The above uncertainties are expected to be addressed in the future to achieve a more realistic and accurate biomass burning emission inventory and a further improvement of model prediction for haze pollution in China. We also plan to explore the crop residue burning effect on a seasonal and annual perspective to better understand its long term contribution to chemical compositions and air quality.

ACKNOWLEDGEMENTS

This study was supported by the National Key R&D Program of China (no. 2017YFC0209802) and the National Natural Science Foundation of China (no. 91644217, no. 41375151).

REFERENCES

Akagi, S.K., Yokelson, R.J., Wiedinmyer, C., Alvarado, M.J., Reid, J.S., Karl, T., Crounse, J.D. and Wennberg, P.O. (2011). Emission factors for open and domestic biomass burning for use in atmospheric models. *Atmos. Chem. Phys.* 11: 4039–4072.

Andreae, M.O. and Merlet, P. (2001). Emission of trace gases and aerosols from biomass burning. G*lobal Biogeochem. Cycles* 15: 955–966.

Badarinath, K.V.S., Kharol, S.K., Sharma, A.R. and Krishna Prasad, V. (2009). Analysis of aerosol and carbon monoxide characteristics over Arabian Sea during crop residue burning period in the Indo-Gangetic Plains using multi-satellite remote sensing datasets. *J. Atmos. Sol. Terr. Phys.* 71: 1267–1276.

Chen, F. and Dudhia, J. (2001). Coupling an advanced land surface-hydrology model with the Penn State-NCAR MM5 modeling system. Part I: Model implementation and sensitivity. *Mon. Weather Rev.* 129: 569–585.

Chen, F., Zhang, X., Zhu, X., Zhang, H., Gao, J. and Hopke, P.K. (2017). Chemical characteristics of $PM_{2.5}$ during a 2016 winter haze episode in Shijiazhuang, China. *Aerosol Air Qual. Res.* 17: 368–380.

Cheng, T., Han, Z., Zhang, R., Du, H., Jia, X., Wang, J. and Yao, J. (2010). Black carbon in a continental semi-arid area of Northeast China and its possible sources of fire emission. *J. Geophys. Res.* 115: D23204.

Cheng, Y., Engling, G., He, K.B., Duan, F.K., Ma, Y.L., Du, Z.Y., Liu, J.M., Zheng, M. and Weber, R.J. (2013). Biomass burning contribution to Beijing aerosol. *Atmos. Chem. Phys.* 13: 7765–7781.

Cheng, Z., Wang, S., Fu, X., Watson, J.G., Jiang, J., Fu, Q., Chen, C., Xu, B., Yu, J., Chow, J.C. and Hao, J. (2014). Impact of biomass burning on haze pollution in the Yangtze River Delta, China: A case study in summer 2011. *Atmos. Chem. Phys.* 14: 4573–4585.

Chou, M.D. and Suarez, M.J. (1994.) An efficient thermal infrared radiation parameterization for use in general circulation models. *NASA Tech. Memo* 104606: 85.

Chuang, M.T., Fu, J.S., Lee, C.T., Lin, N.H., Gao, Y., Wang, S.H., Sheu, G.R., Hsiao, T.C., Wang, J.L., Yen, M.C., Lin, T.H. and Thongboonchoo, N. (2016). The Simulation of long-range transport of biomass burning plume and short-range transport of anthropogenic pollutants to a mountain observatory in East Asia during the 7-SEAS/2010 Dongsha experiment. *Aerosol Air Qual. Res.* 16: 2933–2949.

Crutzen, P.J. and Andreae, M.O. (1990). Biomass burning

in the tropics: Impact on atmospheric chemistry and biogeochemical cycles. *Science* 250: 1669–1678.

Gadde, B., Bonnet, S., Menke, C. and Garivait, S. (2009). Air pollutant emissions from rice straw open field burning in India, Thailand and the Philippines. *Environ. Pollut.* 157: 1554–1558.

Grell, G.A. and Dévényi, D.A. (2002). A generalized approach to parameterizing convection combining ensemble and data assimilation techniques. *Geophys. Res. Lett.* 29: 1693.

Grell, G.A., Peckham, S.E., Schmitz, R., McKeen, S.A., Frost, G., Skamarock, W.C. and Eder, B. (2005). Fully coupled "online" chemistry within the WRF model. *Atmos. Environ.* 39: 6957–6975.

Guenther, A. (2006). Estimates of global terrestrial isoprene emissions using MEGAN (Model of Emissions of Gases and Aerosols from Nature). *Atmos. Chem. Phys.* 6: 3181–3210.

Hong, S.Y. and Pan, H.L. (1996). Nonlocal boundary layer vertical diffusion in a medium-range forecast model. *Mon. Weather Rev.* 124: 2322–2339.

Huang, X., Li, M., Li, J. and Song, Y. (2012). A high-resolution emission inventory of crop burning in fields in China based on MODIS Thermal Anomalies/Fire products. *Atmos. Environ.* 50: 9–15.

Jiang, X., Wiedinmyer, C. and Carlton, A.G. (2012). Aerosols from fires: An examination of the effects on ozone photochemistry in the Western United States. *Environ. Sci. Technol.* 46: 11878–11886.

Koppmann, R., von Czapiewski, K. and Reid, J.S. (2005).A review of biomass burning emissions, Part I: Gaseous emissions of carbon monoxide, methane, volatile organic compounds, and nitrogen containing compounds. *Atmos. Chem. Phys.* 5: 10455–10516.

Langmann, B., Duncan, B., Textor, C., Trentmann, J. and van der Werf, G.R. (2009). Vegetation fire emissions and their impact on air pollution and climate. *Atmos. Environ.* 43: 107–116.

Li, H., Han, Z., Cheng, T., Du, H., Kong, L., Chen, J., Zhang, R. and Wang, W. (2010). Agricultural fire impacts on the air quality of Shanghai during summer harvest time. *Aerosol Air Qual. Res.* 10: 95–101.

Li, X., Wang, S., Duan, L., Hao, J., Li, C., Chen, Y. and Yang, L. (2007). Particulate and trace gas emissions from open burning of wheat straw and corn stover in China. *Environ. Sci. Technol.* 41: 6052–6058.

Li, X., Xia, X., Song, J., Wu, Y., Zhang, X. and Zhang, R. (2017). A case study of long-range transport of smoke aerosols from Eastern Siberia to Northeast China in July 2014. *Aerosol Air Qual. Res.* 17: 965–974.

Lin, Y.L., Farley, R.D. and Orville, H.D. (1983). Bulk parameterization of the snow field in a cloud model. *J. Clim. Appl. Meteorol.* 22: 1065–1092.

Long, X., Tie, X., Cao, J., Huang, R., Feng, T., Li, N., Zhao, S., Tian, J., Li, G. and Zhang, Q. (2016). Impact of crop field burning and mountains on heavy haze in the North China Plain: A case study. *Atmos. Chem. Phys.* 16: 9675–9691.

McMeeking, G.R., Kreidenweis, S.M., Lunden, M., Carrillo, J., Carrico, C.M., Lee, T., Herckes, P., Engling, G., Day, D.E., Hand, J., Brown, N., Malm, W.C. and Collett, J.L. (2006). Smoke-impacted regional haze in California during the summer of 2002. *Agric. For. Meteorol.* 137: 25–42.

Mittal, S.K., Singh, N., Agarwal, R., Awasthi, A. and Gupta, P.K. (2009). Ambient air quality during wheat and rice crop stubble burning episodes in Patiala. *Atmos. Environ.* 43: 238–244.

Mlawer, E.J., Taubman, S.J., Brown, P.D., Iacono, M.J. and Clough, S.A. (1997). Radiative transfer for inhomogeneous atmospheres: RRTM, a validated correlated-k model for the longwave. *J. Geophys. Res.* 102: 16663–16682.

Mukai, S., Yasumoto, M. and Nakata, M. (2014). Estimation of biomass burning influence on air pollution around Beijing from an aerosol retrieval model. *Sci. World. J.* 2014: 10.

Tang, H., Liu, G., Zhu, J., Han, Y. and Kobayashi, K. (2013). Seasonal variations in surface ozone as influenced by Asian summer monsoon and biomass burning in agricultural fields of the northern Yangtze River Delta. *Atmos. Res.* 122: 67–76.

Tao, M., Chen, L., Wang, Z., Tao, J. and Su, L. (2013). Satellite observation of abnormal yellow haze clouds over East China during summer agricultural burning season. *Atmos. Environ.* 79: 632–640.

Tsay, S.C., Maring, H.B., Lin, N.H., Buntoung, S., Chantara, S., Chuang, H.C., Gabriel, P.M., Goodloe, C.S., Holben, B.N., Hsiao, T.C., Hsu, N.C., Janjai, S., Lau, W.K.M., Lee, C.T., Lee, J., Loftus, A.M., Nguyen, A.X., Nguyen, C.M., Pani, S.K., Pantina, P., Sayer, A.M., Tao, W.K., Wang, S.H., Welton, E.J., Wiriya, W. and Yen, M.C. (2016). Satellite-surface perspectives of air quality and aerosol-cloud effects on the environment: An overview of 7-SEAS/BASELInE. *Aerosol Air Qual. Res.* 16: 2581–2602.

Wang, J., Ge, C., Yang, Z., Hyer, E.J., Reid, J.S., Chew, B.N., Mahmud, M., Zhang, Y. and Zhang, M. (2013). Mesoscale modeling of smoke transport over the Southeast Asian Maritime Continent: Interplay of sea breeze, trade wind, typhoon, and topography. *Atmos. Res.* 122: 486–503.

Wang, L., Xin, J., Li, X. and Wang, Y. (2015). The variability of biomass burning and its influence on regional aerosol properties during the wheat harvest season in North China. *Atmos. Res.* 157: 153–163.

Wiedinmyer, C., Akagi, S.K., Yokelson, R.J., Emmons, L.K., Al-Saadi, J.A., Orlando, J.J. and Soja, A.J. (2011). The Fire INventory from NCAR (FINN): A high resolution global model to estimate the emissions from open burning. *Geosci. Model Dev.* 4: 625–641.

Wiedinmyer, C., Quayle, B., Geron, C., Belote, A., McKenzie, D., Zhang, X., O'Neill, S. and Wynne, K.K. (2006). Estimating emissions from fires in North America for air quality modeling. *Atmos. Environ.* 40: 3419–3432.

Wild, O., Zhu, X. and Prather, M.J. (2000). Fast-J: Accurate simulation of in-and below-cloud photolysis in tropospheric chemical models. *J. Atmos. Chem.* 37: 245–282.

Yang, S., He, H., Lu, S., Chen, D. and Zhu, J. (2008). Quantification of crop residue burning in the field and its influence on ambient air quality in Suqian, China. *Atmos. Environ.* 42: 1961–1969.

Yang, W., Wang, G. and Bi, C. (2017). Analysis of long-range transport effects on $PM_{2.5}$ during a short severe haze in Beijing, China. *Aerosol Air Qual. Res.* 17: 1610–1622.

Yao, L., Yang, L.X., Yuan, Q., Yan, C., Dong, C., Meng, C.P., Sui, X., Yang, F., Lu, Y.L. and Wang, W.X. (2016). Sources apportionment of $PM_{2.5}$ in a background site in the North China Plain. *Sci. Total Environ.* 541: 590–598.

Zaveri, R.A. and Peters, L.K. (1999). A new lumped structure photochemical mechanism for large-scale applications. *J. Geophys. Res.* 104: 30387–30415.

Zaveri, R.A., Easter, R.C., Fast, J.D. and Peters, L.K. (2008). Model for simulating aerosol interactions and chemistry (MOSAIC). *J. Geophys. Res.* 113: 1395–1400.

Zhang, R., Jing, J., Tao, J., Hsu, S.C., Wang, G., Cao, J., Lee, C.S.L., Zhu, L., Chen, Z., Zhao, Y. and Shen, Z. (2013). Chemical characterization and source apportionment of $PM_{2.5}$ in Beijing: Seasonal perspective. *Atmos. Chem. Phys.* 13: 7053–7074.

Zhang, F., Wang, J., Ichoku, C., Hyer, E.J., Yang, Z., Ge, C., Su, S., Zhang, X., Kondragunta, S. and Kaiser, J.W. (2014). Sensitivity of mesoscale modeling of smoke direct radiative effect to the emission inventory: A case study in northern sub-Saharan African region. *Environ. Res. Lett.* 9: 075002.

Zhang, T., Claeys, M., Cachier, H., Dong, S., Wang, W., Maenhaut, W. and Liu, X. (2008). Identification and estimation of the biomass burning contribution to Beijing aerosol using levoglucosan as a molecular marker. *Atmos. Environ.* 42: 7013–7021.

Zhu, B., Su, J., Han, Z., Yin, C. and Wang, T. (2010). Analysis of a serious air pollution event resulting from crop residue burning over Nanjing and surrounding regions. *China Environ. Sci.* 30: 585–592.

Received for review, September 27, 2017
Revised, January 15, 2018
Accepted, January 15, 2018